A Neural Model of the Fly Visual System Applied to Navigational Tasks

Cyrill Planta, Jörg Conradt, Adrian Jencik, Paul Verschure

Institute of Neuroinformatics, Winterhurerstrasse 190, 8057 Zuerich, Switzerland

Abstract. We investigate how elementary motion detectors (EMDs) can be used to control behavior. We have developed a model of the fly visual system which operates in real time under real world conditions and was tested in course and altitude stabilization tasks using a flying robot. While the robot could stabilize gaze i.e. orientation, we found that stabilizing translational movements requires more elaborate preprocessing of the visual input and fine tuning of the EMDs. Our results show that in order to control gaze and altitude EMD information needs to be computed in different processing streams.

1 Introduction

Flies possess an elaborated visual system that supports their fast and accurate flying maneuvers. Whenever the relative position or orientation of the fly to the world changes, a global change of the illuminance distribution occurs, called optic flow. Optic flow fields of different movements such as rotation (yaw), translation, or moving upwards or downwards (lift) may resemble each other within limited areas of the visual field, but never across the entire field of view. Flies are believed to exploit optical flow by calculating the local image movements among their visual field with EMDs and integrate these signals. This processing takes place in the wide-field integrating (WF) neurons, cells with large dendritic trees whose receptive fields match certain optic flow fields ([4]).
In order to understand how EMD information is used in motor control, robots have been constructed which use EMDs and WF neurons to detect rotational egomotion and avoid obstacles (e.g. [2], [7] ,[3]). However very few researchers (e.g. [3]) have started to investigate whether the same concepts also work for robots moving in three dimensions and what the requirements are when movements other than rotational egomotions need to be detected. To address these questions we have built a flying robot capable of moving in three dimensions. The robot was controlled by a neural network which is a model of the fly visual system. We analyzed the robot's behavior in a course and altitude stabilization task, during which the trajectory, the WF neurons's responses, and the optomotor signals were recorded and analyzed (See figure 1A).

2 Methods

Robot: The robot was constructed using a blimp with a payload of 120 g. We attachedtwo b/w cameras laterally on the surface of the blimp with a field of view of 56° x 42° (Fig. 1A(d)). We mounted four motors with propellers on the ventral side of the blimp (Fig. 1A(c)). Two propellers were aligned in the horizontal plane and two in the vertical plane. The propellers could drive the robot forward at a speed of up to 3m/s

and rotate it with an angular velocity of up to 112°/s. We used three radio links to exchange the onboard robot data with the neural network. Each camera had a separate video transmitter and the propellers were controlled by a third radio communication module (Fig. 1A(e)).

3D Tracking: In order to analyze the behavior of the robot accurately we tracked both the position and the orientation of the robot online. Two ceiling cameras (Fig. 1A(a)) were tracking two IR emitting diode arrays mounted on top of the blimp (Fig. 1A(b)). The transition from the two camera pixel coordinates into a pair of three dimensional coordinates was achieved by a multilayer perceptron. The tracking resolution yielded an accuracy of 5cm.

Software: We used the simulation software IQR421 [6] to implement and control the neural model, the 3D tracking and the robot. For data analysis we used both IQR421 and Matlab.

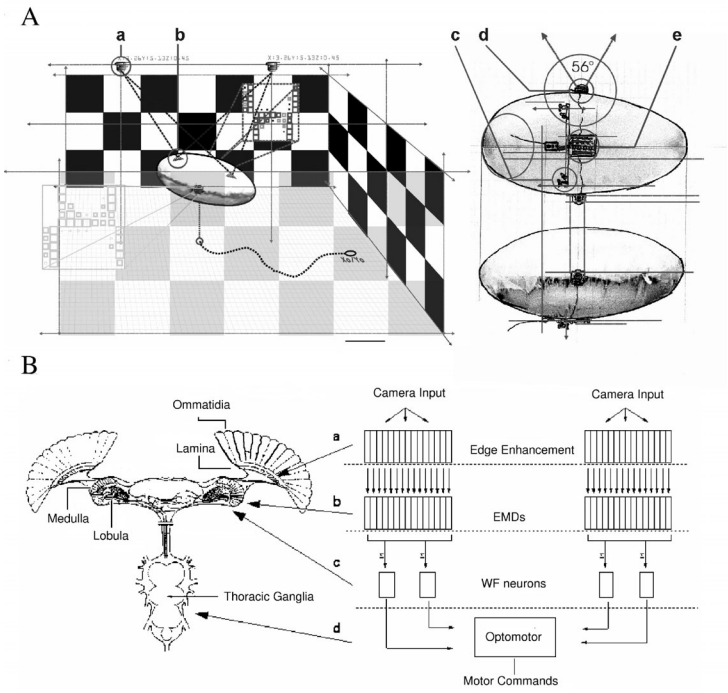

Fig. 1. A: The experimental setup and the robot. The robot moves freely in 3D being tracked by ceiling cameras (a). Visual input stems from two cameras atached laterally on the blimp (d). Checkerboard patterns are attached on the walls and the ground in order to enhance contrast. The neural network steering the robot resides on a PC and communicates via radio links with the robot (see text for further details). B: Schematic of the model. See text for explanation (Left part is adapted from [1]).

3 Model

Figure 1B gives an overview of how the fly visual system was modeled. Initially the camera image was downscaled to a resolution of 10x10 pixels. This image was the input for cells with center-surround receptive fields whose basic function was to enrich contrasts in the image similar to the function of laminar processing (Fig.1 Ba). The resulting image was then relayed to four distinct groups of EMDs which computed the four elementary motions using the Reichhardt correlation model [8]. In the fly this processing is thought to take place presynaptically to the lobular cells (Fig.1 B(b)). Like the large lobular cells the WF neurons had distinct large dendrites and integrated the responses of the EMDs (Fig.1 B(c)). There were two WF cells sensitive to left and right rotation and two that were sensitive to up or down translation. Finally all the WF neurons responses from the two processing streams were integrated and transduced linearly into a motor signal (Fig.1 B(d)). This motor signal was directed against the dominating type of movement, i.e. when a left rotation was sensed the robot rotates right and vice versa. If the WF neurons responses were below a certain threshold the robot flew forward. 2647 linear threshold neurons and 3800 synapses were needed to build the model.

4 Results

4.1 General Behavior

In order to understand whether the model could control flight behavior we analyzed in detail the relationship between neuronal responses and motor actions in figure 2A. To begin with we wanted to know how and how often the robot makes use of its neural network. Figure 2A describes the relevant processes in the robot and the trajectory of the robot when moving through the experimental room (the whole trajectory can be seen in inset (a)). Starting at the beginning of the big arrow in figure 2A(b) we see that the robot senses left rotation and compensates with right rotation commands. This is followed with a moment of no rotation being sensed. After that the robot senses a tiny right rotation (too small to be visible) and overcompensates until it finds itself in a state of left rotation. Again the robot compensates to the right; at the end of the big arrow no rotation is sensed by the robot. Over a distance of one meter the direction of rotation and the compensating motor command changes four times, showing that the neural network continously controls the behavior of the robot which results in trajectories that form straight lines.

4.2 Yaw Compensation

In a first experiment we examined whether the wide-field integration of EMDs provides useful information for the robot to compensate for unintended course deviations while traveling through the experimental room. The performance was measured as the average angular speed of the robot, its average deviation from course. In this experiments the two cameras were placed laterally on the blimp and only horizontal optical flow was processed. In the control condition the robot would simply fly with both horizontal motors turned on, relying on its aerodynamics.
The robot with the EMD model enabled performed significantly better than the control (an average angular velocity of 1.7(+/- 0.4)°/s, versus 16.2(+/- 0.6)°/s in the control

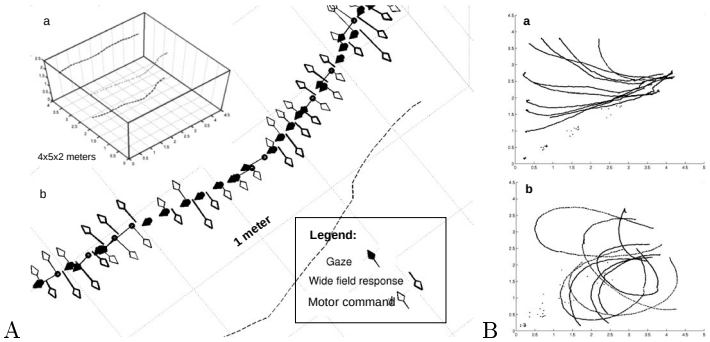

Fig. 2. A: Typical 3D trajectory of the robot. (a): overall trajectory. (b): Close up on (a). Filled black arrows visualize gaze and velocity (length of arrow); thick perpendicular arrows show the directioned sum of the WF neurons responses, where an arrow on the right of the gaze arrow means that the robot senses right rotation and vice versa. Thin arrows denote direction and strength of the current motor command (when no motor command is visible, the robot is flying forwards). These arrows point in the opposite direction of the WF arrows in order to compensate for the rotation. B: Overlaid 2D trajectories of course stabilization experiments. (a) Model enabled, (b) model disabled.

condition). Figure 2B shows the overlaid two dimensional trajectories of experiments with the model enabled (a) and disabled (b). Although the robot cannot maintain its initial gaze it can still pursue a stable course (Fig. 2 B(a)) whereas in the control condition, once the robot has rotational momentum it does not recover from such deviations (Fig. 2 B(b)). This shows that the model can reliably compensate for course deviations.

4.3 Altitude Control

The next step was to test whether the robot could control its altitude and whether the EMD and WF neuron concept could be extended to altitude stabilization. We analyzed two configurations of how such a task could be implemented in our model. In the first configuration (lateral) the cameras were attached laterally on the blimp and the responses of vertically tuned EMDs's were integrated and transformed into a compensating motor response. In the other configuration (ventral) we attached the cameras on the ventral surface of the robot (inspired by [5]) and tuned the EMDs to be sensitive to forward motion in the ventral field of view. In this case when translating forwards a uniform optic flow field exists in the ventral part of the robot's field of view. Because optic flow for close objects is larger than for objects further apart, the optic flow increases when the robot approaches the ground.
Figure 3A shows the robot's height, the sum of the relevant WF neuron activities, and the upward motor response over time. Both the motor response and and the EMD response increase as the altitude of the blimp drops. The robot detects that it is approaching ground and triggers the upward motor command. In the following analysis we only focus on the robot's fundamental ability to "sense" a change in altitude.
After testing different delay values of the EMDs in both configurations in order to

find the maximum sensitivity of the EMDs for lift we evaluated whether the lateral configuration was suitable for altitude control. To answer this question we calculated the ratio of correct "upwards" decisions versus wrong upwards "decisions". We also determined whether and how this ratio improves if the robot only makes decisions when the WF neuron signals are above a certain signal threshold. Finally we wanted to see how much information has to be thrown away when such a threshold is used. Figure 3B(a) summarizes this data. The maximum correct/wrong ratio which has the value of 1 in figure 3B(a) was 28. However in this case the robot would only exploit 1 percent of the information available. When no signal threshold is used the correct/wrong ratio lies around chance level.
Figure 3 B(b) shows the same ratios for the ventral configuration. The ratio between correct and wrong decisions was lower than in the lateral configuration whereby the maximum in the plot stand for a correct/wrong ratio of 9.
This data suggests that the accuracy of altitude control using EMDs depends on their specific tuning and this accuracy can be increased by tresholding the signal strength.

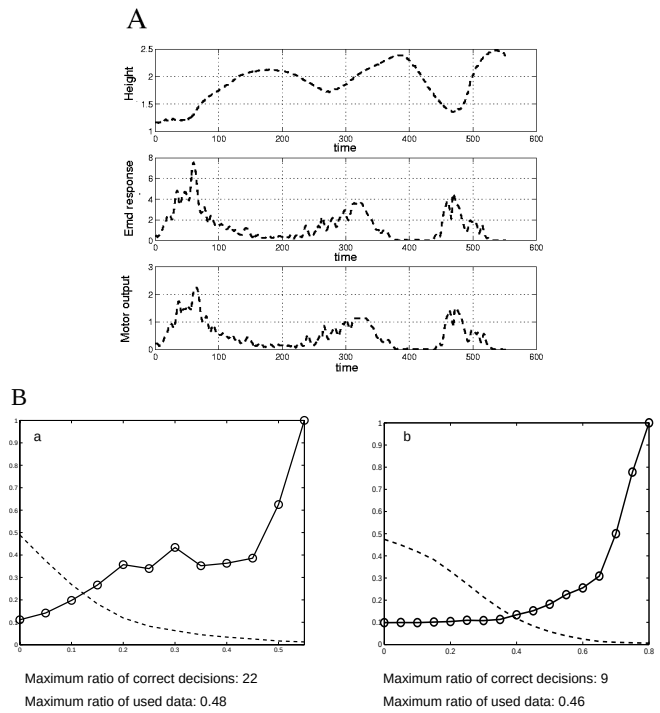

Fig. 3. A: Time course of Height, EMD response, and motor output. B: All curves are normalized in respect to their maximum value which is shown below the plots. (a) The solid curve shows the normalized ratio of correct up judgment to wrong up judgments of the robot in the lateral configuration. The dashed curve shows the ratio of data which was used for a judgement. The x-axis values are the signal tresholds. (b) Correct/wrong ratios and ratio of unused data for the ventral configuration.

5 Discussion

We have investigated a model of the fly visual system with the aim to understand how EMD signals can be integrated in order to achieve reliable 3D control of a flying robot. We have analyzed the behavior of the robot in a rotational course compensation task in several runs. Furthermore we evaluated the responses of WF neurons in two configurations of an altitude stabilization task in open loop experiments.
The robot performed well in the course compensation task. This is in accordance with the performance of various insectoid robots ([2], [3]) and also with the performance of other flying robots ([3]). In contrast to these robots our solution used a smaller field of view (two times 56°x42° in our case, versus nearly surround views in [2] and [3]) and also a simpler preprocessing of the image before the EMDs. This emphasizes the robustness of the EMD concept whenever there is a high amount of optical flow to process, as is the case when we want to detect rotational egomotion.
On the perceptual level we saw that the EMD concept is stretched to its limits when we tried to estimate lift, which is a translational motion and elicits less optical flow than rotation. The fine tuning of EMD's and the application of a signal threshold yielded better results at the cost of discarding potentially useful information. The performance in judging its lift was better in the lateral than in the ventral configuration. One would have assumed that the configuration wich sees more optic flow would be more reliable, namely the ventral configuration. Hence the underlying cause of these results requires further investigation. Nevertheless we can conclude that if EMDs are used for the detection of translatory motion they need a specific tuning and signal thresholds need to be used for accurate judgements. Hence different processing streams are required to solve both rotational and translational compensation tasks.

References

1. M. Egelhaaf and A. Borst. Motion Computation and Visual Orientation in Flies. *Comp. Biochem. Physiol.*, 10:659–673, 1993.
2. Franchescini, J.M. Pichon, and C Blanes. From insect vision to robot vision. *Phil. Trans. R. Soc. Lond. B*, 1992.
3. F. Iida. Goal-directed navigation of an automonus flying robot using biologically inspired cheap vision. *Proceedings of the 32nd ISR*, 2001.
4. H.G. Krapp. Neuronal matched filters for optic flow processing inflying insects. *International review of neurobiology*, 44:93–120, 2000.
5. T.R. Neumann and H.H. Buelthoff. Biologically motivated visual control of attitude and altitude in translatory flight. *Proceedings of the 3rd Workshop Dynamische Perzeption Ulm/Germany*, 2000.
6. P. Verschure. Iqr421: A software tool for synthesis and analysis of neural systems. *Techn. Report, Institute of Neuroinformatics ETH/University Zurich*, 1997.
7. K. Weber, S. Venkatesh, and M.V. Srinivasan. Insect inspired behaviours for the automonous control of mobile robots. *From Living Eyes to Seeing Machines.*, pages 227–248, 1997.
8. J.M. Zanker and M. Egelhaaf. Speed tuning in elementary motion detectors of the correlation type,. *Biological Cybernetics*, 80:109–116, 1999.